Valence-Band Mixing Effects in the Upper-Excited-State Magneto-Optical Responses of Colloidal Mn^{2+}-Doped CdSe Quantum Dots

Rachel Fainblat,*,† Franziska Muckel,† Charles J. Barrows,‡ Vladimir A. Vlaskin,‡ Daniel R. Gamelin,‡ and Gerd Bacher†

†Werkstoffe der Elektrotechnik and CENIDE, University Duisburg-Essen, Bismarckstraße 81, Duisburg, 47057 Germany and ‡Department of Chemistry, University of Washington, Seattle, Washington 98195-1700, United States

ABSTRACT We present an experimental study of the magneto-optical activity of multiple excited excitonic states of manganese-doped CdSe quantum dots chemically prepared by the diffusion doping method. Giant excitonic Zeeman splittings of each of these excited states can be extracted for a series of quantum dot sizes and are found to depend on the radial quantum number of the hole envelope function involved in each transition. As seven out of eight transitions involve the same electron energy state, $1S_e$, the dominant hole character of each excitonic transition can be identified, making use of the fact that the *g*-factor of the pure heavy-hole component has a different sign compared to pure light hole or split-off components. Because the magnetic exchange interactions are sensitive to hole state mixing, the giant Zeeman splittings reported here provide clear experimental evidence of quantum-size-induced mixing among valence-band states in nanocrystals.

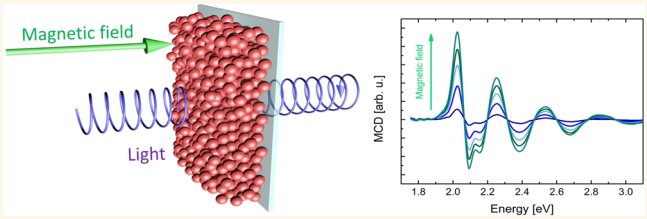

KEYWORDS: diluted magnetic semiconductors · nanocrystals · valence-band mixing · excited states · sp−d exchange interaction

The three-dimensional confinement of quantum dots is expected to cause significant valence-band mixing,[1−4] resulting in a large number of excitonic transitions of mixed hole character. This scenario is in distinct contrast to that of, for example, two-dimensional systems, which show no such mixing. Valence-band mixing has been suggested to affect important physical properties of quantum dots, such as piezoelectric fields,[5,6] phonon modes of excited states,[7] polarization degree,[8] spin dephasing,[9] spin-selective tunneling,[10] and magneto-optical response,[11] all of which are relevant to the potential technological utility of this class of materials. To date, however, there has been no experimental demonstration of valence-band mixing in the upper excited states of quantum dots.

Unique access to the important size-dependent perturbation of valence-band mixing can be achieved by exploring the excitonic Zeeman splittings of higher excited states in magnetically doped quantum dots. Doping semiconductors with paramagnetic transition-metal ions introduces strong dopant-carrier sp−d magnetic exchange coupling that leads to the so-called "giant" excitonic Zeeman effect.[12−18] Magnetic exchange interactions can enhance excitonic Zeeman splittings by roughly 2 orders of magnitude, offering a strong magneto-optical response that is sensitive to the excitonic wave function. In general, the giant Zeeman splitting ($\Delta E_{sp\text{-}d}$) of an exciton in a cubic semiconductor is proportional to $N_0(\alpha + \mathbf{n} \times \beta)$, with a weighting factor $\mathbf{n}$ depending on the valence subband involved in the exciton transition. Here, N_0 is the cation density, and α and β are mean-field exchange parameters. For the heavy hole (hh) $\mathbf{n} = -1$, whereas $\mathbf{n} = +1/3$ for the light hole (lh) and $\mathbf{n} = +2/3$ for the split-off (so) hole.[18] The sign and amplitude of $\Delta E_{sp\text{-}d}$ thus depend on the specific valence subband involved. The most commonly investigated excitonic state is related to the band-edge transition and involves a heavy

* Address correspondence to Rachel.fainblat-padua@uni-due.de.

Received for review October 2, 2014 and accepted December 1, 2014.

Published online December 01, 2014
10.1021/nn505610e

hole (hh-X). Some work has described the giant Zeeman splittings of lh-X transitions in epilayers,[19,20] multiquantum wells,[21,22] and colloidal nanoribbons.[23] Even in highly quantum confined two-dimensional structures such as these, the description of $\Delta E_{sp\text{-}d}$ introduced above remains valid, because to a first approximation their quantum confinement does not induce valence-band mixing. Previous magneto-optical studies of diluted magnetic semiconductor (DMS) quantum dots have been restricted to just the lowest excitonic state,[17,24−27] which is not noticeably affected by valence-band mixing, except for the case of a strongly anisotropic shape.[28]

Here we report magneto-optical measurements of the giant Zeeman splittings of multiple upper excited states in magnetically doped quantum dots. Specifically, we analyze the magneto-optical responses of a large number of excitonic transitions in colloidal Mn^{2+}-doped CdSe quantum dots of different sizes using magnetic circular dichroism (MCD) spectroscopy. By focusing on the Zeeman splittings of upper excitonic states, the measurements described here provide an experimental test of the assumption of pure hole character that is usually invoked for analyzing the giant Zeeman effect in bulk materials and two-dimensional systems. Our results show that this assumption is valid only for particular excited states in quantum dots, *i.e.*, those that are not affected by valence-band mixing, offering new insights into the fundamental electronic structures of semiconductor quantum dots.

The measurements described here were performed on colloidal CdSe nanocrystals doped with Mn^{2+} ions *via* the recently reported diffusion-doping method.[29] This method has the advantage that the seed nanocrystals can be grown independently with very narrow size distributions, prior to doping. Here, we show that the nanocrystals prepared by this method display exceptionally well resolved upper excited states in their absorption and MCD spectra, providing the unique opportunity to evaluate the properties of these upper excited states in detail.

RESULTS AND DISCUSSION

For the results reported here, we prepared samples of nanocrystals with different diameters and different Mn^{2+} concentrations. Sample 1 has a diameter of 5.9 nm and contains 2.5% (cation mole percent) Mn^{2+}. Samples 2 and 3 are 5.4 and 4.8 nm in diameter, containing 0.4% and 1% (cation mole percent) Mn^{2+}, respectively. The samples are predominantly in the cubic crystallographic phase (~100% cubic in the case of sample 1 and ~65% and ~85% cubic for samples 2 and 3, respectively), as determined by X-ray diffraction measurements (see Supporting Information). Thin films of these nanocrystals were prepared by drop casting the nanocrystal dispersions onto quartz substrates. Magnetic circular dichroism measurements

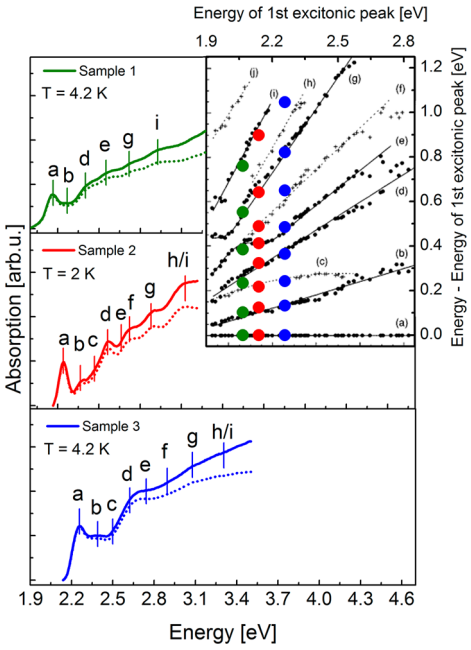

Figure 1. Solid lines: Absorption of samples 1 (green), 2 (red), and 3 (blue). Dotted lines represent the absorption data, where the background stemming from light scattering is subtracted. Inset: Comparison between the calculations/experiments of Norris *et al.*[3] and the energetic positions of the different excitonic peaks of samples 1 to 3 (full circles). This comparison allows assignment of the transitions labeled by a to i according to the notation introduced in the text. Assignment: (a) $1S_{3/2}1S_e$, (b) $2S_{3/2}1S_e$, (c) $1S_{1/2}1S_e$, (d) $1P_{3/2}1P_e$, (e) $2S_{1/2}1S_e$, (f) $1P_{5/2}1S_e/1P^{l}_{1/2}1S_e$, (g) $3S_{1/2}1S_e$, (h) $1S_{1/2}1D_e/2S_{1/2}2S_e/1S_{1/2}2S_e/2S_{3/2}1D_e/1D_{5/2}1D_e/4P_{3/2}1P_e$, (i) $4S_{3/2}2S_e/1S_{1/2}2S_e/1P^{so}_{1/2}1S_e$.

were performed using a self-made setup measuring the differential absorption of right and left circularly polarized light of a sample placed in an external magnetic field in the Faraday geometry. With this setup, we are able to measure both the absorption and the MCD spectrum simultaneously.

The solid lines in Figure 1 represent the measured absorption spectra of samples 1, 2, and 3 (green, red, and blue, respectively). The excellent size distribution achieved *via* diffusion doping allows the observation of multiple excitonic transitions despite the spectral broadening that accompanies doping.[29] Due to nanocrystal agglomeration in the thin films, the measured absorption is a superposition of the real absorption and light scattering. Comparing the absorbance of a thin film sample with and without an integrating sphere, we determined that at higher energies the light scattering accounts for about 20% of the total absorbance. To correct for this, we subtracted the scattering (proportional to $1/\lambda^4$) from the raw data, yielding the dotted lines in Figure 1. All three samples exhibit at least six excitonic transitions, which were assigned according to the notation of Norris and Bawendi.[3] Note that a precise determination of the energy position of each absorption peak is achieved by analyzing the positions of the minima of the second

derivative of the absorption spectra (see Supporting Information).

Using the effective mass model, Norris *et al.*[3] predicted the energy positions of multiple excitonic transitions in CdSe quantum dots with different sizes. In this context, each charge carrier is described using spherical harmonics and Bessel functions due to the three-dimensional confinement. The notation n_eL_e of the electron envelope function contains its angular momentum L_e and the radial quantum number n_e. In contrast to the electrons, the valence-band holes are affected by mixing between subbands (heavy hole, light hole, and split-off hole: hh, lh, and so), and the hole characters of the excited states are not clearly defined as in the case of bulk materials or quantum wells. The hole states n_hL_F of the quantum dots are described by the quantum number F (total hole angular momentum), which is a sum of the angular momentum L_h and J (total unit cell angular momentum). An exception from the valence-band mixing occurs in the case of the P-like hole states, allowing the occurrence of pure light hole ($1P_{1/2}^{l}$) or split-off hole ($1P_{1/2}^{so}$) states.

The inset of Figure 1 plots the energetic positions of the excitonic features observed in the absorption spectra of our samples, in comparison to the calculations/experiments of Norris and coauthors.[3] A very good agreement is seen, allowing assignment of each excitonic transition. These assignments are summarized in the caption of Figure 1. Not all excitonic transitions exhibit the same oscillator strength; for example, transitions **c**, **f**, and **h** exhibit lower oscillator strengths than the other ones. Because of the nanocrystal size distribution, not all excitonic features are well resolved in every sample. For example, feature **c** does not appear in the absorption spectrum of sample 1 and **e/f** and **g/h** are not distinguishable. Because the oscillator strength of **h** is expected to be lower than that for **g**, we assume that the observed feature mainly originates from transition **g** in this case. In the case of sample 2, the excitonic features are more clearly separated and all transitions from **a** to **g** can be assigned. The last excitonic peak of sample 2 is between the expected energies for **h** and **i**; that is, the transitions are not distinguishable. An even stronger quantum confinement enables the clear assignment of all peaks from **a** to **h** for sample 3.

Figure 2 plots the MCD spectra of the same three samples, each measured at several magnetic fields. Several pronounced magneto-optical features are observed in the spectral range of the assigned absorption peaks. The total MCD signal in any spectrum is a superposition of multiple MCD features, and it is therefore necessary to separate the contributions of each transition in order to extract Zeeman splittings from such data. The first step in the data analysis is a fit of the absorption peaks, which is shown in the bottom of

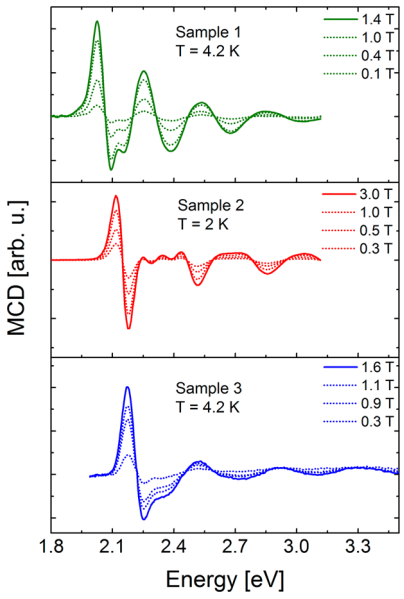

Figure 2. MCD spectra of samples 1 (green), 2 (red), and 3 (blue) for different magnetic fields. The magneto-optical activity of several excitonic transitions can be seen clearly.

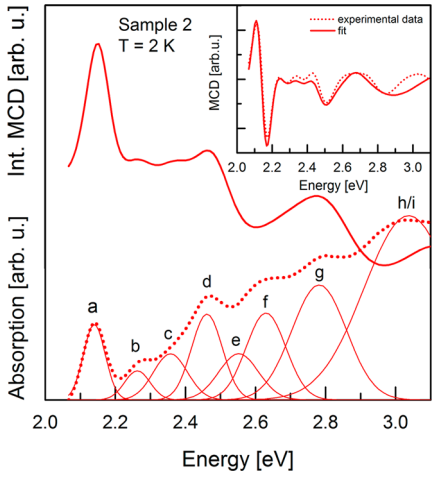

Figure 3. Bottom: Absorption without background of sample 2 (dotted line) and fitted Gaussian peaks of multiple excitonic transitions from a to h/i (solid lines). Top: Integral of the measured MCD spectrum for determination of the sign of the Zeeman splitting of each excitonic transition. Inset: Comparison between the experimental data (dotted line) and the simulated MCD spectrum.

Figure 3 for sample 2. To a good approximation, a given MCD feature is describable as the first derivative of the corresponding absorption peak.[30] Moreover, the line shape of the MCD feature reflects the sign of the excited-state Zeeman splitting; for a negative (positive) Zeeman splitting, we expect a positive (negative) MCD peak followed by a negative (positive) one with increasing energy. Note, these signs depend on the convention used to define the MCD signal. In our case, if the effective g-factor of the excitonic state is positive (negative), the Zeeman splitting is negative (positive), consistent with the convention used previously.[4,31]

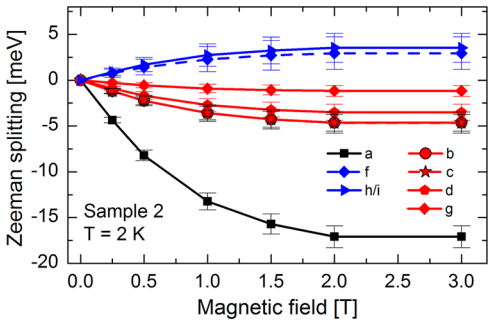

Figure 4. Zeeman splittings extracted from the MCD signal of sample 2 for multiple excitonic transitions. The transitions with low oscillator strength are represented by dashed lines. As expected, the band-edge excitonic transition (a) exhibits the largest splitting. Two transitions (f and h/i) exhibit a positive Zeeman splitting, which indicates dominant lh or so character of the involved hole states. The amplitude of the Zeeman splitting of the transitions b, c, d, and g lie between the two limiting cases, as evidence of valence-band mixing.

These properties allow the signs of the Zeeman splittings to be determined from the MCD data: if the integrated MCD signal ($\int_{E_{min}}^{E_{max}}$MCD(E) dE) yields a maximum (minimum) at the energy of the absorption peak, the Zeeman splitting is negative (positive). Combining the determined sign of the Zeeman splitting of the nth excited state and the derivative of the corresponding absorption peak, the total MCD spectrum can be simulated using eq 1 with the amplitudes of the Zeeman splittings as the only fitting parameters.

$$\mathrm{MCD_{tot}}(E) = \sum_{n=a}^{i} \Delta E_n \frac{\mathrm{d}\{[\mathrm{Abs}(E)]_n\}}{\mathrm{d}E} \qquad (1)$$

The MCD signal obtained from this fitting procedure is shown with the experimental data in the inset of Figure 3. The simulated MCD spectrum is in good agreement with the measured data, allowing extraction of the magnetic-field-dependent Zeeman splitting of each individual excitonic transition.

Figure 4 plots the Zeeman splittings of the different excited states *versus* magnetic field determined for sample 2. The excitonic transitions with an expected lower oscillator strength are plotted using dashed lines. The error bars for the nth transition were estimated based on the deviation between the simulated and the measured MCD data by the variation of ΔE_n as a single-fit parameter (see equation above). On the basis of the amplitudes and the signs of the Zeeman splittings, we can separate the different excited states into three groups: the band-edge excitonic transition **a**, the transitions **f** and **h/i** with a positive Zeeman splitting, and several transitions (**b**, **c**, **d**, and **g**) showing a negative Zeeman splitting. The band-edge excitonic transition $1S_{3/2}1S_e$ (**a**) is dominantly heavy-hole-like[2] and therefore exhibits the largest negative Zeeman splitting. In contrast, there are two transitions exhibiting a positive sign (**f** and **h/i**) in the Zeeman splitting. More interesting, two of these excitons show no valence-band mixing, containing pure light hole (**f** contains $1P^{I}_{1/2}1S_e$) or split-off hole character (**i** contains $1P^{so}_{1/2}1S_e$), both expected to exhibit an opposite sign compared to their heavy hole counterparts. Hence, we can conclude that the light hole or split-off hole character plays an important role in the magneto-optical responses of states **f** and **h/i**, respectively.

The Zeeman splittings of the other excitonic transitions (**b**, **c**, **d**, and **g**) are comparable in magnitude to one another and between the two limiting cases. It is thus obvious that impure hole states are involved, and valence-band mixing must play a central role. Interestingly, the Zeeman splittings of the transitions with the same total hole angular momentum F and same angular momentum L_h decrease with increasing radial quantum number n_h, which is to first order related to the quantization energy. We therefore attribute this trend to an increased mixing of the valence-band states; compare **a** ($1S_{3/2}1S_e$) and **b** ($2S_{3/2}1S_e$) or **c** ($1S_{1/2}1S_e$) or **g** ($3S_{1/2}1S_e$).

It is instructive to compare the results of some selected excitonic transitions for different samples. In Figure 5, Zeeman splittings of all well-resolved transitions are plotted for all three samples. To simplify the comparison and exclude the influence of different dopant concentrations, the values of $\Delta E_{sp\text{-}d}$ for each transition have been normalized by the absolute value of transition **a** at the magnetic field of 1.7 T for that sample.

Although the MCD measurements of the different samples were performed at slightly different temperatures (2 K *vs* 4.2 K, compare the curvatures of the Zeeman data for both samples), transition **a** exhibits the largest Zeeman splitting in all cases, as expected due to the dominant heavy hole character. Transitions **b**, **d**, **e**, and **g** are representative of the second group, exhibiting strongly mixed hole character. Interestingly, the normalized amplitudes of the Zeeman splittings of these transitions decrease with increasing quantum confinement (compare samples 1 to 3). The Zeeman splitting related to transition **f** is positive for samples 2 and 3, in accordance with theoretical expectations for the pure light-hole-like transition $1P^{I}_{1/2}1S_e$. In the case of sample 1, transitions **e** and **f** are superimposed, and **f** cannot be resolved because of its lower oscillator strength. It is difficult to draw a clear conclusion about transitions **h** and **i**, since they are not distinguishable for all samples. Only in the case of sample 1 is transition **i** spectrally well resolved, exhibiting a negative Zeeman splitting, while for samples 2 and 3 we observe a superposition of both **h** and **i**, with an overall positive Zeeman splitting. According to theory, one might expect the Zeeman splitting of transition **i** to be positive due to the split-off character of the involved $1P^{so}_{1/2}1S_e$ state. Nevertheless, **i** contains two further transitions affected by the valence-band mixing, which

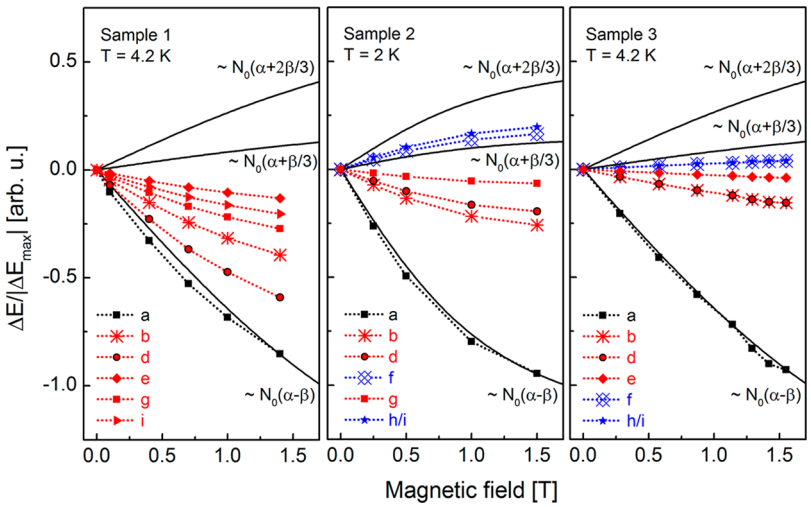

Figure 5. Experimental values of the Zeeman splittings (dotted lines) for samples 1, 2, and 3, normalized by the absolute value of the respective transition a at 1.7 T. For comparison, the theoretical curves expected for purely heavy-hole, light-hole, and split-off excitonic transitions are plotted (black solid lines) normalized at the magnetic field of 1.7 T. The error bars of all transitions lie within the same range as shown in Figure 4 and were intentionally omitted here for better clarity.

may explain the deviation between this theoretical expectation and the experimental data. The fact that in both samples 2 and 3 the superposition of **h** and **i** exhibits an apparent positive Zeeman splitting allows the conclusion that **h** is probably dominated by light hole and/or split-off character.

In the next step, we compare the experimental data with the theoretical expectation of excitonic transitions exhibiting pure hole character, which is proportional to the Brillouin function B_S:[32]

$$\Delta E \propto AB_S\left(\frac{g\mu_B SB}{k_B(T+T_0)}\right)$$

Here, g represents the dopant g-factor (2.004 for Mn^{2+} in CdSe), μ_B the Bohr magneton, S the total dopant spin (in the case of Mn^{2+}, $S = 5/2$), B the magnetic field, k_B the Boltzmann constant, and T the sample temperature. T_0 is related to an effective sample temperature due to antiferromagnetic coupling between dopants. The prefactor A depends on the character of the hole involved, with $A_{hh} = N_0(\alpha-\beta)$ for the heavy hole exciton, $A_{lh} = N_0(\alpha+\beta/3)$ for the light hole exciton, and $A_{so} = N_0(\alpha + 2\beta/3)$ for the split-off hole,[18] for cubic crystal lattices. In this quantum dot size range, the bulk parameters ($N_0\alpha = +0.23$ eV and $N_0\beta = -1.27$ eV in the case of bulk $Cd_{1-x}Mn_xSe$[33]) can be used for the exchange constants.[34]

For quantum dots in the studied size range, the band-edge excitonic transition is mostly heavy-hole-like.[2] The fact that transitions **b**, **d**, **e**, and **g** lie between the theoretical curves for hh-X and lh-X/so-X is evidence of the increasing valence-band mixing. As seen in Figure 5, the experimental data of **f** and **h/i** are in qualitative agreement with the theoretical expectation for excitonic transitions with dominant lh-X and so-X character, respectively. Note that a quantitative agreement cannot be expected here because, on one hand, even the exciton ground state might not be of pure heavy hole character as assumed for the theoretical curves, and in addition, the **h/i** transition might involve P-like electron ($4P_{3/2}1P_e$) or D-like electron or hole states ($1S_{1/2}1D_e/2S_{3/2}1D_e/1D_{5/2}1D_e$). Nevertheless, this experimental result suggests such additional effects are relatively small. Overall, our data clearly show how the different valence-band hole character (hh, lh, so) of the different excitonic states in DMS quantum dots yields different magneto-optical responses, and the data further provide a clear illustration of deviations from the idealized behavior of these upper-excited-state Zeeman splittings due to quantum-confinement-induced valence-band mixing.

CONCLUSIONS

In summary, the magneto-optical responses of multiple excitonic states have been measured and analyzed in a series of colloidal DMS quantum dots. From the Zeeman splitting data, three characteristic groups of optical transitions can be separated: (i) the heavy hole dominated band-edge excitonic transition, (ii) two transitions exhibiting a positive Zeeman splitting, and (iii) transitions with a Zeeman splitting between these two limiting cases. Comparing the experimental data with theoretical predictions, we were able to identify the dominant hole character (heavy, light, and split-off) of each excited state. Analysis of these data yields clear evidence of pronounced confinement-induced valence-band mixing in upper excitonic states of colloidal CdSe quantum dots, and the impact of this mixing on the magnitudes and even signs of upper-excited-state excitonic Zeeman splittings in doped quantum dots is described. This work provides

new insights into the electronic structures and physical properties of semiconductor nanocrystals. These insights are rooted in fundamental principles, and as such should be generalizable across the entire class of zero-dimensional nanostructures subject to confinement-induced valence-band mixing.

METHODS

Determination of the Crystal Structure. XRD data were collected using a Bruker D8 Discover spectrometer at the University of Washington NanoTech User Facility.

Magnetic Circular Dichroism. Our MCD setup consists of an excitation source, a modulator for polarization of the excitation light, and a photomultiplier for the detection. The wavelength-tunable light source is based on a 75 W xenon lamp and a monochromator (LOT Oriel, 1200 grooves/mm grating blazed at 500 nm). The modulation between right and left circularly polarized light at a frequency of 50 kHz is realized using a combination of a linear polarizer and a photoelastic modulator. The sample is placed in a helium cryostat in the presence of a variable magnetic field (Faraday geometry). Due to interaction of the energy levels and the applied magnetic field, the sample will absorb right (σ^+) or left (σ^-) circularly polarized light differently, originating an MCD signal, which is proportional to Abs(σ^+) − Abs(σ^-), where Abs represents the absorption of the sample. A photomultiplier (model R928, Hamamatsu) detects the transmitted light, whose dc (ac) component is read out using an HP 34401A multimeter (lock-in amplifier Signal Recovery 7225 DSP).

Conflict of Interest: The authors declare no competing financial interest.

Supporting Information Available: Determination of the crystal structure, experimental setup, and assignment of energetic position of higher excited states. This material is available free of charge *via* the Internet at http://pubs.acs.org.

Acknowledgment. We are grateful to the Deutsche Forschungsgemeinschaft under contract Ba 1422/13 for financial support. This work was supported in part by the U.S. National Science Foundation through DMR-1206221 (D.R.G.).

REFERENCES AND NOTES

1. Ekimov, A. I.; Hache, F.; Schanne-Klein, M. C.; Ricard, D.; Flytzanis, C.; Kudryavtsev, I. A.; Yazeva, T. V.; Rodina, A. V.; Efros, A. L. Absorption and Intensity-Dependent Photoluminescence Measurements on CdSe Quantum Dots: Assignment of the First Electronic Transitions. *J. Opt. Soc. Am. B* **1993**, *10*, 100.
2. Chen, P. Quantum Shape Effects on Zeeman Splittings in Semiconductor Nanostructures. *Phys. Rev. B* **2005**, *72*, 045335.
3. Norris, D. J.; Bawendi, M. G. Measurement and Assignment of the Size-Dependent Optical Spectrum in CdSe Quantum Dots. *Phys. Rev. B* **1996**, *53*, 16338.
4. *Semiconductor Quantum Dots*; Klimov, V. I., Ed.; CRC Press: Boca Raton, FL, 2010.
5. Jiang, Z.-J.; Kelley, D. F. Surface Charge and Piezoelectric Fields Control Auger Recombination in Semiconductor Nanocrystals. *Nano Lett.* **2011**, *11*, 4067.
6. Plumhof, J. D.; Trotta, R.; Křápek, V.; Zallo, E.; Atkinson, P.; Kumar, S.; Rastelli, A.; Schmidt, O. G. Tuning of the Valence Band Mixing of Excitons Confined in GaAs/AlGaAs Quantum Dots *via* Piezoelectric-Induced Anisotropic Strain. *Phys. Rev. B* **2013**, *87*, 075311.
7. Kelley, A. M. Electron-Phonon Coupling in CdSe Nanocrystals from an Atomistic Phonon Model. *ACS Nano* **2011**, *5*, 5254.
8. Chekhovich, E. A.; Krysa, A. B.; Skolnick, M. S.; Tartakovskii, A. I. Direct Measurement of the Hole-Nuclear Spin Interaction in Single InP/GaInP Quantum Dots Using Photoluminescence Spectroscopy. *Phys. Rev. Lett.* **2011**, *106*, 027402.
9. Kaji, R.; Ohno, S.; Hozumi, T.; Adachi, S. Effects of Valence Band Mixing on Hole Spin Coherence *via* Hole-Nuclei Hyperfine Interaction in InAlAs Quantum Dots. *J. Appl. Phys.* **2013**, *113*, 203511.
10. Katsaros, G.; Golovach, V. N.; Spathis, P.; Ares, N.; Stoffel, M.; Fournel, F.; Schmidt, O. G.; Glazman, L. I.; De Franceschi, S. Observation of Spin-Selective Tunneling in SiGe Nanocrystals. *Phys. Rev. Lett.* **2011**, *107*, 246601.
11. Durnev, M. V.; Glazov, M. M.; Ivchenko, E. L.; Jo, M.; Mano, T.; Kuroda, T.; Sakoda, K.; Kunz, S.; Sallen, G.; Bouet, L.; *et al.* Magnetic Field Induced Valence Band Mixing in [111] Grown Semiconductor Quantum Dots. *Phys. Rev. B* **2013**, *87*, 085315.
12. Hoffman, D. M.; Meyer, B. K.; Ekimov, A. I.; Merkulov, I. A.; Efros, Al. L.; Rosen, M.; Couino, G.; Gacoin, T.; Boilot, J. P. Giant Internal Magnetic Fields in Mn Doped Nanocrystal Quantum Dots. *Solid State Commun.* **2000**, *114*, 547.
13. Beaulac, R.; Schneider, L.; Archer, P. I.; Bacher, G.; Gamelin, D. R. Light-Induced Spontaneous Magnetization in Doped Colloidal Quantum Dots. *Science* **2009**, *325*, 973.
14. Pandey, A.; Brovelli, S.; Viswanatha, R.; Li, L.; Pietryga, J. M.; Klimov, V. I.; Crooker, S. A. Long-Lived Photoinduced Magnetization in Copper-Doped ZnSe-CdSe Core-Shell Nanocrystals. *Nat. Nanotechnol.* **2012**, *7*, 792.
15. Beaulac, R.; Archer, P. I.; Ochsenbein, S. T.; Gamelin, D. R. Mn^{2+}-Doped CdSe Quantum Dots: New Inorganic Materials for Spin-Electronics and Spin-Photonics. *Adv. Funct. Mater.* **2008**, *18*, 3873–389.
16. Bryan, J. D.; Gamelin, D. R. In *Progress in Inorganic Chemistry*, Karlin, K. D., Ed.; John Wiley & Sons: NJ, 2005; Vol. 54, pp 47−126.
17. Bussian, D. A.; Crooker, S. A.; Yin, M.; Brynda, M.; Efros, A. L.; Klimov, V. I. Tunable Magnetic Exchange Interactions in Manganese-Doped Inverted Core-Shell ZnSe-CdSe Nanocrystals. *Nat. Mater.* **2009**, *8*, 35.
18. Gaj, J. A. In *Semiconductors and Semimetals*; Furdyna, J. K.; Kossut, J., Eds.; Academic Press: San Diego, 1988; Vol. 25, pp 275−309.
19. Yu, W.; Twardowski, A.; Fu, L.; Petrou, A.; Jonker, B. Magnetoanisotropy in $Zn_{1-x}Mn_xSe$ Strained Epilayers. *Phys. Rev. B* **1995**, *51*, 9722.
20. Pacuski, W.; Ferrand, D.; Cibert, J.; Deparis, C.; Gaj, J.; Kossacki, P.; Morhain, C. Effect of the s,p-d Exchange Interaction on the Excitons in $Zn_{1-x}Co_xO$ Epilayers. *Phys. Rev. B* **2006**, *73*, 035214.
21. Peyla, P.; Wasiela, A.; Merle d'Aubigné, Y.; Ashenford, D.; Lunn, B. Anisotropy of the Zeeman Effect in $CdTe/Cd_{1-x}Mn_xTe$ Multiple Quantum Wells. *Phys. Rev. B* **1993**, *47*, 3783.
22. Kuhn-Heinrich, B.; Ossau, W.; Bangert, E.; Waag, A.; Landwehr, G. Zeeman Pattern of Semimagnetic (CdMn)Te/(CdMg)Te Quantum Wells in Inplane Magnetic Fields. *Solid State Commun.* **1994**, *91*, 413.
23. Fainblat, R.; Frohleiks, J.; Muckel, F.; Yu, J. H.; Yang, J.; Hyeon, T.; Bacher, G. Quantum Confinement-Controlled Exchange Coupling in Manganese(II)-Doped CdSe Two-Dimensional Quantum Well Nanoribbons. *Nano Lett.* **2012**, *12*, 5311.
24. Norris, D. J.; Yao, N.; Charnock, F. T.; Kennedy, T. A. High-Quality Manganese-Doped ZnSe Nanocrystals. *Nano Lett.* **2001**, *1*, 3.
25. Archer, P. I.; Santangelo, S. A.; Gamelin, D. R. Direct Observation of sp-d Exchange Interactions in Colloidal Mn^{2+}- and Co^{2+}-Doped CdSe Quantum Dots. *Nano Lett.* **2007**, *7*, 1037.
26. Norberg, N. S.; Parks, G. L.; Salley, G. M.; Gamelin, D. R. Giant Excitonic Zeeman Splittings in Colloidal Co^{2+}-Doped ZnSe Quantum Dots. *J. Am. Chem. Soc.* **2006**, *128*, 13195.

27. Schimpf, A. M.; Gamelin, D. R. Thermal Tuning and Inversion of Excitonic Zeeman Splittings in Colloidal Doped CdSe Quantum Dots. *J. Phys. Chem. Lett.* **2012**, *3*, 1264.
28. Léger, Y.; Besombes, L.; Maingault, L.; Mariette, H. Valence-Band Mixing in Neutral, Charged, and Mn-Doped Self-Assembled Quantum Dots. *Phys. Rev. B* **2007**, *76*, 045331.
29. Vlaskin, V. A.; Barrows, C. J.; Erickson, C. S.; Gamelin, D. R. Nanocrystal Diffusion Doping. *J. Am. Chem. Soc.* **2013**, *135*, 14380.
30. Stephens, P. Theory of Magnetic Circular Dichroism. *J. Chem. Phys.* **1970**, *52*, 3489.
31. Kuno, M.; Nirmal, M.; Bawendi, M. G.; Efros, A.; Rosen, M. Magnetic Circular Dichroism Study of CdSe Quantum Dots. *J. Chem. Phys.* **1998**, *108*, 4242.
32. Gaj, J. A.; Planel, R.; Fishman, G. Relation of Magneto-Optical Properties of Free Excitons to Spin Alignment of Mn^{2+} Ions in $Cd_{1-x}Mn_xTe$. *Solid State Commun.* **1979**, *29*, 435.
33. Madelung, O.; Rössler, U.; Schulz, M. In *Numerical Data and Functional Relationships in Science and Technology*; Landolt-Börnstein, Group III, Condensed Matter Vol. 41B; Springer Verlag: New York, 1999.
34. Beaulac, R.; Feng, Y.; May, J. W.; Badaeva, E.; Gamelin, D. R.; Li, X. Orbital Pathways for Mn^{2+}-Carrier sp-d Exchange in Diluted Magnetic Semiconductor Quantum Dots. *Phys. Rev. B* **2011**, *84*, 195324.